Newton's cradles in optics: From *N*-soliton fission to soliton chains

R. Driben,[1,2,*] B. A. Malomed,[1] A. V. Yulin,[3] and D. V. Skryabin[4]

[1]*Department of Physical Electronics, School of Electrical Engineering, Faculty of Engineering, Tel Aviv University, Tel Aviv 69978, Israel*

[2]*Department of Physics CeOPP, University of Paderborn, Warburger Straße 100, D-33098 Paderborn, Germany*

[3]*Centro de Fisica Teorica e Computacional, Faculdade de Ciencias, Universidade de Lisboa, Avenida Professor Gama Pinto 2, Lisboa 1649-003, Portugal*

[4]*Department of Physics, University of Bath, Bath BA2 7AY, United Kingdom*

A mechanism for creating a Newton's cradle (NC) in nonlinear light wave trains under the action of the third-order dispersion (TOD) is demonstrated. The formation of the NC structure plays an important role in the process of fission of higher-order (*N*) solitons in optical fibers. After the splitting of the initial *N* soliton into a nonuniform chain of fundamental quasisolitons, the tallest one travels along the entire chain, through consecutive collisions with other solitons, and then escapes, while the remaining chain of pulses stays as a bound state, due to the radiation-mediated interaction between them. Increasing the initial soliton's order, *N*, leads to the transmission through, and release of additional solitons with enhanced power, along with the emission of radiation, which may demonstrate a broadband supercontinuum spectrum. The NC dynamical regime remains robust in the presence of extra perturbations, such as the Raman and self-steepening effects, and dispersion terms above the third order. It is demonstrated that essentially the same NC mechanism is induced by the TOD in finite segments of periodic wave trains (in particular, soliton chains). A difference from the mechanical NC is that the TOD-driven pulse passing through the soliton array collects energy and momentum from other solitons. Thus, uniform and nonuniform arrays of nonlinear wave pulses offer an essential extension of the mechanical NC, in which the quasiparticles, unlike mechanical beads, interact inelastically, exchanging energy and generating radiation. Nevertheless, the characteristic phenomenology of NC chains may be clearly identified in these nonlinear-wave settings too.

PACS number(s): 42.81.Dp, 42.65.Tg, 05.45.Yv

I. INTRODUCTION

Beyond its natural manifestations in various mechanical systems [1], the commonly known Newton-cradle (NC) setup (which was actually first built, as an experimental device, by French physicist Edme Mariotte in 1670 [2]) has found microscopic realizations in atomic and molecular chains [3]. Another physically interesting possibility is to build NCs as a chain of solitons or wave pulses, if they may be considered as repulsively interacting quasiparticles. This option was elaborated in detail in terms of an immiscible binary Bose-Einstein condensate, assuming that the chain is built as a string of alternating solitons composed of mutually repelling components, while the intrinsic nonlinearity of each component is self-attractive [4]. Still earlier, a similar system was studied experimentally and theoretically in the form of "supersolitons" in a chain of magnetic-flux quanta (fluxons) pinned to a lattice of defects in a long Josephson junction [5]. Very recently, it was reported that a finite chain of *dissipative solitons* in a two-dimensional model of the laser cavity, with a built-in spatially periodic grating, may also feature an NC dynamical regime, if the trapped chain is initially hit by a moving soliton [6]. Characteristic features of the NC phenomenology are clearly observed in that setting, even if the underlying dynamics is dissipative, being governed by a complex Ginzburg-Landau equation.

In the present work we aim to present a realization of the NC in nonlinear optical fibers, where the "cradle," in the form of a nonuniform train of quasisolitons, is naturally produced as a result of the fission of *N*th-order solitons (*N*-solitons) under the action of the third-order dispersion (TOD). The process of higher-order-soliton fission is, by itself, of great significance to applications (see below). It will be demonstrated that the realization of the NC array in this setting is vastly different from the classical chain of identical hard beads: The constituent solitons have different sizes, and they interact inelastically, exchanging energy and emitting considerable amounts of radiation. Nevertheless, the overall dynamical scenario may be identified as that characteristic to NC systems: The uttermost soliton starts the motion from the left edge of the array, which triggers a localized wave of the energy and momentum transfer across the array, ending up with the release of one or several free solitons from the right edge, while the other solitons stay in the form of a bound chain. In fact, these results suggest that the NC concept is not restricted to the mechanical realizations, and may be extended to more general settings. In fact, an essential extension suggested by the present results is that colliding quasiparticles may effectively *pass through each other* in the NCs based on soliton arrays.

It is well known that, in addition to the ubiquitous fundamental solitons, the integrable nonlinear Schrödinger (NLS) equation and physical systems described by nearly integrable versions of this equation [7] support *N*-soliton states, with $N \geqslant 2$, which are oscillating modes periodically restoring their shape at distances that are multiples of the fundamental soliton period [8]. Although they are subject to a weak splitting instability, due to the fact that their binding energy is equal to zero, in the case of the integrable equation (the splitting may be catalyzed by a weak resonant periodic modulation of the nonlinearity strength [9]), higher-order

*driben@post.tau.ac.il

solitons were observed in nonlinear optical fibers [10], and robust $N = 2$ solitons have been created as basic modes in soliton lasers [11]. Recently, dynamics of higher-order solitons was studied theoretically in regular and parity-time-symmetric nonlinear dual-core couplers [12].

The fission of N solitons in nonlinear optical fibers is naturally caused by higher-order linear and nonlinear effects [13–16], such as the Raman-induced self-frequency shift [17,18], self-steepening [19], and TOD, which are included into the corresponding generalized NLS equations [20,21]. The point at which the fission occurs is, usually, the one where the bandwidth of the evolving N-soliton attains its maximum. On the other hand, the oscillations of the N-soliton in its unperturbed form can be naturally used for strong compression of the pulse (the so-called soliton-compression effect) [22,23]. The fission of higher-order solitons is a key enabling mechanism for the generation of ultrashort frequency-tuned fundamental solitons [24], and for the creation of ultrabroadband supercontinuum [21,25]. Recent advances in manufacturing photonic-crystal fibers filled with Raman-inactive gases [26] provide an additional motivation to focus the studies on the TOD-induced fission and its potential applications to photonics, in the absence of the Raman effect.

In earlier works, it was demonstrated that higher-order terms, treated as small perturbations, split N-solitons into a set of N different fundamental solitons, with the sequence of peak powers analytically predicted by the well-known exact solution of Satsuma and Yajima [see Eq. (3) below [8,14]]. However, we demonstrate below that, when the input pulse is injected close to the zero-dispersion point, hence the TOD effect is relatively strong, such a simple picture of the soliton fission is far from reality and a detailed numerical study is required.

The rest of the paper is structured as follows. The model is formulated in Sec. II, which is followed by the presentation of the main numerical results in Sec. III. As mentioned above, the results demonstrate that the fission of N solitons under the action of the TOD proceeds via the creation of NCs in the form of nonuniform soliton chains, and passage of one or several tallest solitons across the entire chain, ending by release of the passing solitons, while the remaining ones stay in the form of bound array. An essential difference of the NC dynamical regime in the soliton arrays from the NC in chains of mechanical particles is that collisions of solitons are partly inelastic, in the nonintegrable system. As a result, the passing soliton collects additional energy and momentum from the other pulses, and is eventually released from the array with a considerable increase of the energy, and with a large frequency shift. To demonstrate the relevance of the generalized NC concept in the broader context of nonlinear optics, in Sec. IV we demonstrate the realization of the TOD-driven NC in periodic patterns of wave pulses, such as "prefabricated" chains of identical solitons. The paper is concluded by Sec. IV.

II. THE MODEL

The dynamics of ultrashort pulses in nonlinear fibers is governed by the generalized NLS equation for amplitude A of the electromagnetic field, which includes the TOD, self-

steepening, and Raman terms [20,21]:

$$\frac{\partial A}{\partial z} = \sum_{m \geqslant 2} \frac{i^{m+1}\beta_m}{m!} \frac{\partial^m A}{\partial T^m} + i\gamma\left(1 + \frac{i}{\omega_0}\frac{\partial}{\partial T}\right)$$
$$\times \left[A(z,\tau)\int_{-\infty}^{T} d\tau' \, R(T - T')|A(z,T')|^2\right], \quad (1)$$

where, as usual, z and and T are the propagation distance and reduced time [20], and β_m is the mth-order dispersion coefficient at carrier frequency ω_0. The fiber loss is neglected in Eq. (1), as the fission of the N-soliton and formation of the NC occur on the propagation-distance scale which is much shorter than the absorption length. Further, the nonlinearity coefficient is taken as $\gamma = 0.08$ W^{-1} m^{-1}, and the response function is $R(T) = (1 - f_R)\delta(T) + f_R h_R(T)$, with the first and second terms standing for the instantaneous and delayed (Raman) contributions, respectively. Here $f_R = 0.18$ is the fraction of the Raman contribution to the nonlinear polarization, and $h_R(\tau) = [(\tau_1^2 + \tau_2^2)/(\tau_1\tau_2^2)]\exp(-T/\tau_2)\sin(T/\tau_1)$ approximates the Raman response function of the silica fiber [19], with $\tau_1 = 12.2$ fs and $\tau_2 = 32$ fs. Hereafter, the second-order group-velocity-dispersion (GVD) coefficient is taken as $\beta_2 = -0.0021$ ps^2/m, with the pulse injected at carrier wavelength $\lambda = 800$ nm into the anomalous-GVD region of the fiber, close to the zero-dispersion point (ZDP).

Equation (1) was solved numerically by means of the split-step Fourier method [20]. Actually, the simulations of the N-soliton fission included the Raman effect and the shock term only at the last stage of the analysis, the results of which are displayed below in Figs. 6 and 7 to show that these terms are not crucially important for the NC dynamics, unlike the TOD. Higher-order-dispersion terms, up to the seventh order, are also included in simulations presented in Fig. 7. As mentioned above, neglecting the Raman self-frequency shift is relevant, in particular, for the pulse propagation in holey fibers filled by Raman-inactive gases [26], where the effective Raman coefficient is four or five orders of magnitude smaller than in silica.

III. N-SOLITON FISSION VIA THE NEWTON-CRADLE MECHANISM

Simulations of Eq. (1) were performed with the input in the form of the usual N-soliton,

$$u(z = 0, T) = N\sqrt{P_0}\text{sech}(T/T_0), \quad (2)$$

with $N > 1$, and by setting $T_0 = 50$ fs (the respective FWHM width is ≈ 90 fs). With the above-mentioned value of the second-order GVD coefficient $\beta_2 = -0.0021$ ps^2/m, the peak power of the fundamental soliton corresponding to this width is $P_0 = 10.5$ W. While the second-order dispersion parameter is kept constant, its third-order counterpart (the TOD coefficient) will be varied. In the case of weak TOD, the analysis of the N-soliton splitting, based on the perturbation theory, was developed in Ref. [14]. However, for larger values of β_3, the dynamics is more complex, strongly deviating from the prediction of the perturbative analysis (see Fig. 4 below). The TOD distorts the fundamental pulse, making it asymmetric, with a periodic oscillatory structure emerging near one edge [20,27], which results from dispersive waves and is described by the Airy function [28]. Accordingly, the shape of the
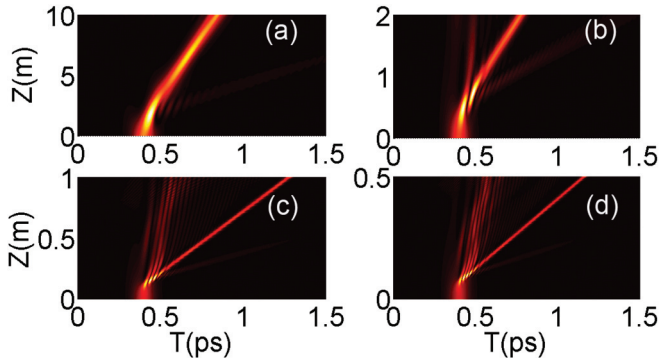
FIG. 1. (Color online) The fission dynamics of the $N = 1.5$ soliton (a), $N = 3$ soliton (b), $N = 5$ soliton (c), and $N = 10$ soliton (d). The simulations of Eq. ((1)) with $\beta_3 = 6.98 \times 10^{-5}$ ps³/m were performed for input (2) with $T_0 = 50$ fs and $P_0 = 10.55$ W.

soliton experiences a strong deformation with the appearance of this oscillating structure at the front or rear side of the soliton [20], depending on the sign of β_3. Here we consider the case of opposite signs of the TOD and second-order GVD (for identical signs, the results can be obtained by substitution $T \rightarrow -T$, which reverses the sign of β_3).

Despite the fact that the energy coupled into the radiation under the action of TOD is relatively small, it was demonstrated that the dispersive wave carries away a significant amount of momentum [29]. The periodic light structure at the edge of the pulse induces effective refractive index change, which attracts the main peak of the pulse. If more energy is injected into the fiber than is required for the formation of the fundamental soliton, the interaction between the oscillatory structure and the peak of the pulse becomes stronger, causing acceleration or delay of the pulse. This situation is shown in Fig. 1(a), where input pulse (2) was taken with peak power 23.625 W, corresponding to $N = 1.5$ at $T_0 = 50$ fs.

The injection of larger energy leads to further enhancement of the interaction between the main peak and the oscillatory structure. The first-born tallest soliton starts to advance from the left edge of the wave train to the right under the action of the strong TOD, consecutively colliding with all the other peaks in the emerging chain. Phase shifts $\Delta\varphi$ between adjacent peaks were measured to range in the interval of $\pi/2 < \Delta\varphi < 3\pi/2$, making the collisions between individual pulses repulsive [7]. The colliding pulses exchange the energy and momentum

before the soliton is ejected from the pulse array, carrying extra energy and featuring a frequency shift (i.e., carrying extra momentum), which were accumulated due to nonelasticity of collisions under the action of TOD [30].

Figures 1(b)–1(d) display the dynamical regimes developed from input (2) corresponding to $N = 3$, 5, and 10, with $T_0 = 50$ fs. In the case of the three-soliton input [Fig. 1(b)], the escaping soliton is actually ejected from the second channel of the arrayed structure. Further, the fission of the five-soliton input [Fig. 1(c)] results in the ejection from the third channel, and, in the case of $N = 10$ [Fig. 1(d)], the ejection from the seventh effective channel is observed. In each case, additional pulses, located to the right of the ejecting channel, remain very weak at the moment when the soliton escapes. To further illustrate the NC dynamics following the fission of the $N = 10$ soliton, Fig. 2(a) zooms the area from Fig. 1(d) where the cradle emerges, and Fig. 2(b) displays snapshots of the field's intensity at several values of the propagation distance Z.

While the tallest soliton, driven by the TOD, passes the whole chain from left to right and eventually escapes, the remaining pulses continue the propagation in a bound state. In the case of large values of the TOD coefficient, β_3, the chain mostly stays in the region of the normal second-order GVD, while, with the decrease of β_3, it is shifted mostly to the anomalous-GVD domain, thus increasing the soliton content of the chain. The situation is illustrated by Figs. 3(a) and 3(b) by means of two XFROG diagrams [31], pertaining to $\beta_3 = 6.98 \times 10^{-5}$ ps³/m and $\beta_3 = 1.75 \times 10^{-5}$ ps³/m, respectively. In the former case, the chain [marked by label 2 in Fig. 3(a)] mostly belongs to the normal-GVD region, at $\lambda < \lambda_{ZDP} = 790$ nm. The carrier wavelength of the ejected soliton [marked by 1 in Fig. 3(a)] is shifted to 870 nm, while the radiation component (labeled by 3 in the figure) appears at the blue edge of the spectrum, around $\lambda = 680$ nm. In the case of the weak TOD [$\beta_3 = 1.75 \times 10^{-5}$ ps³/m; see Fig. 3(b)], the chain [its segment is labeled by 2 in Fig. 3(b)] mostly belongs to the anomalous-GVD region, at $\lambda > \lambda_{ZDP} = 761$ nm, hence these pulses may be interpreted as being close to regular solitons. The carrier wavelength of the ejected soliton [marked by 1 in Fig. 3 (b)] is shifted to 930 nm, while the radiation component (labeled 3 in the figure) appears at the blue edge of the spectrum, around $\lambda = 600$ nm.

To characterize the mechanism of the TOD-driven NC formation from the fissile N-solitons, we measured the peak
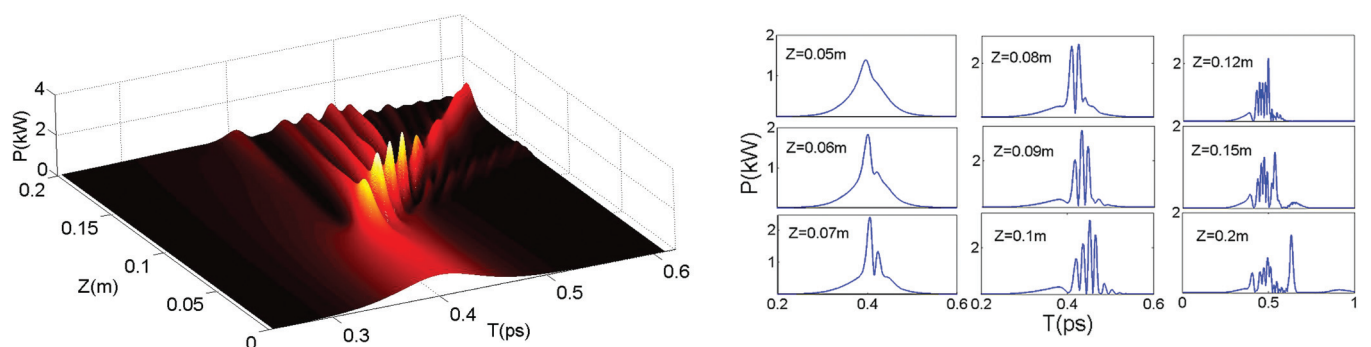

FIG. 2. (Color online) (a) The zoomed three-dimensional view of the fission of the $N = 10$ soliton from Fig. 1(d), in the area where the "cradle" emerges. (b) Snapshots of the evolution of the local-power distribution, $P \equiv |A(z,T)|^2$. The tallest soliton is ejected at $Z \simeq 0.18$ m.
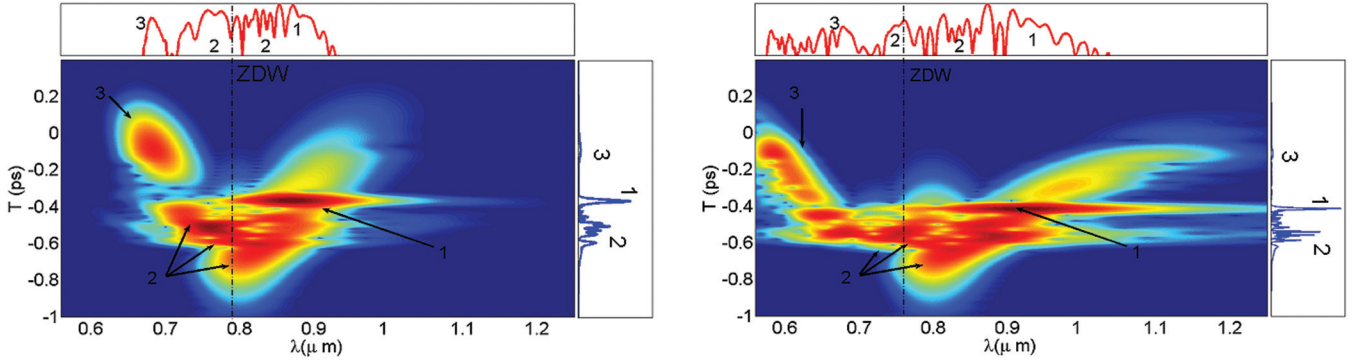
FIG. 3. (Color online) XFROG representation of the ten-soliton-fission dynamics at $Z = 0.2$ m with (a) $\beta_3 = 6.98 \times 10^{-5}$ ps³/m, and (b) $\beta_3 = 1.75 \times 10^{-5}$ ps³/m.

power of the first ejected soliton, as well as its wavelength shift, as a function of the peak power of the originally injected N soliton (2), which is proportional to $N^2 P_0$, while its width was fixed, as said above, to $T_0 = 50$ fs. The results are plotted in Fig. 4 versus order N of the input.

In the case of very weak TOD, the well-known analytical result of Satsuma and Yajima [8] predicts peak powers of fundamental solitons into which the Nth-order one is decomposed:

$$P^{(j)} = P_0(2N - 2j - 1)^2, \quad j = 0,...,N-1, \quad (3)$$

where P_0 is the same as in Eq. (2). This result, if applied to the splitting of the $N = 10$ soliton, shows that the largest peak power in the set of the emerging fundamental solitons should be 3.6 times higher than that of the original N soliton, and the energy carried away by this tallest soliton is about 18% of the total energy of the parental N soliton. However, the relatively strong TOD makes the actual peak power of the escaping soliton significantly lower, as seen in Fig. 4. For example, the fission of the $N = 10$ soliton displayed above produces the free soliton with the peak power of 1 kW, which is only 1.2 times higher than that of the parental $N = 10$ soliton. On the other hand, the energy of the single ejected soliton is about 30% of the initial pulse's energy. The latter result is explained by the
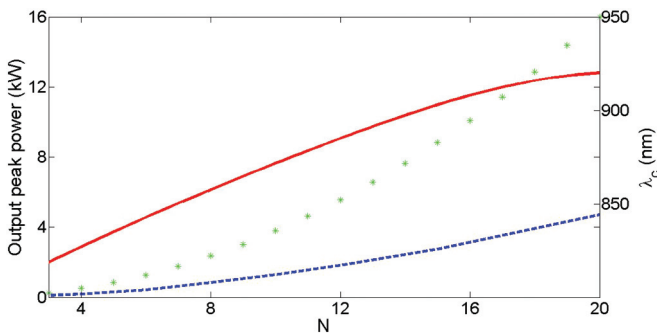
fact that, under the action of the strong TOD, the collisions are not exactly elastic [30], allowing the ejected soliton to collect energy donated by weaker solitons in the course of its travel through the chain.

Due to inelastic effects of the collisions and interaction with the conspicuous radiative component of the field, the escaping soliton experiences additional acceleration (the wavelength shift, which is shown by the solid red curve in Fig. 4). The wavelength shift starts to saturate close to $N = 20$. For even higher orders of N in the input, one can achieve still higher peak-power ratios between the tallest generated soliton and the input, and a somewhat higher frequency shift, but, due to the interaction between the multiple generated solitons and dispersive waves [32], the control over parameters of the generated solitons deteriorates.

At higher values of N (between 10 and 20), the soliton-cradle effect, in the form of a tall pulse passing the chain by dint of consecutive collisions and eventually escaping into the free space, repeats itself several times. After the first soliton has been ejected, the cradle retains enough strength to push additional solitons all the way through the chain, up to the ejection accompanied by conspicuous emission of radiation, as shown in Fig. 5. Reducing the TOD coefficient β_3, which drives the soliton motion through the chain, makes the NC dynamical regime less pronounced, allowing the system to

FIG. 4. (Color online) The wavelength shift of the tallest fundamental soliton generated by the fission of the N-soliton input (2), relative to the input wavelength of 800 nm (the solid red curve), and the peak power of this soliton (the dashed blue curve), vs the input peak power, for $\beta_3 = 6.98 \times 10^{-5}$ ps³/m. For the sake of comparison, the dotted green curve shows the analytical result (3) for the peak power of the tallest soliton in the integrable NLS equation.
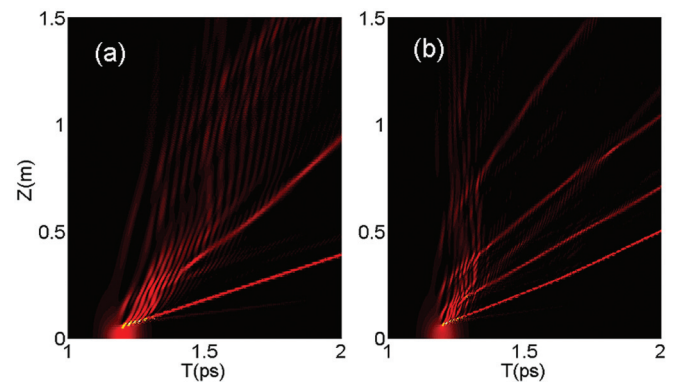

FIG. 5. (Color online) The fission of the 12th-order soliton. (a) The second fundamental soliton is ejected after the first one, at $\beta_3 = 6.98 \times 10^{-5}$ ps³/m. (b) Multiple soliton ejection observed when the TOD strength is reduced to $\beta_3 = 1.74 \times 10^{-5}$ ps³/m.
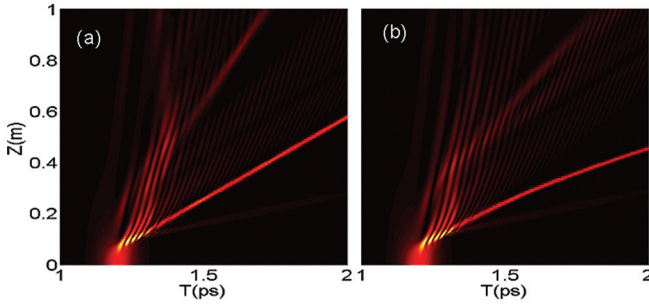
FIG. 6. (Color online) The fission of the $N = 10$ soliton in the presence of the self-steepening (a), and Raman self-frequency shift (b). In either case, the second fundamental soliton is ejected, following the ejection of the first soliton, after the array has passed the propagation distance $Z \simeq 0.5$ m.

increase the number of soliton-ejection cycles, as shown in Fig. 5. The figure demonstrates the fission of the $N = 12$ soliton under the action of $\beta_3 = 6.98 \times 10^{-5}$ ps^3/m (a) and $\beta_3 = 1.74 \times 10^{-5}$ ps^3/m (b). The effect of the multisoliton ejection, along with the emission of dispersive waves, from the initial N soliton with high values of N manifests itself in the generation of broadband supercontinua.

To verify the robustness of the NC dynamical regimes presented above, the simulations of Eq. (1) were reproduced including other higher-order terms, viz., the cubic ones accounting for the self-steepening and the Raman effect. The results demonstrate that the extra terms do not cardinally affect the NC regime and subsequent ejection of the tallest soliton. Actually, the higher-order nonlinear terms somewhat amplify the NC effects, lending the ejected solitons an additional redshift, which is induced by the Raman term. A typical example of the fission of the $N = 10$ soliton in the presence of these additional terms is displayed in Fig. 6, which demonstrates the ejection of additional solitons. It can be compared to the $N = 10$ soliton's fission in Fig. 1(d) with the same input and the same value of the TOD coefficient, $\beta_3 = 6.98 \times 10^{-5}$ ps^3/m, where no ejection of the second soliton was observed for the same propagation length. Generally, the TOD-driven NC regime governs the generation and ejection of the soliton, while its motion in the free space is accelerated by the Raman effect.

It is also relevant to verify the robustness of the NC effect against the addition of higher-order dispersive terms,

which we did by simulating the fission of the N soliton in the framework of the full equation (1) including the dispersive terms of up to the seventh order. The respective dispersion coefficients were taken for the fiber model as per Ref. [15], at the carrier wavelength $\lambda = 800$ nm (while $\lambda_{\mathrm{ZDP}} = 790$ nm): $\beta_2 = -2.1$ fs^2/mm, $\beta_3 = 69.83$ fs^3/mm, $\beta_4 = -73.25$ fs^4/mm, $\beta_5 = 191.9$ fs^5/mm, $\beta_6 = -727$ fs^6/mm, and $\beta_7 = 1549.4$ fs^7/mm. The injected peak power 26.25 kW corresponds to the input's order $N = 50$ (such high values of N are relevant if the objective is the generation of supercontinuum [21,25]). Figures 7(a) and 7(b) demonstrate the corresponding fission process in the temporal and spectral domains, respectively. In Fig. 7(a), one can clearly observe strong signatures of the NC dynamics, in the form of narrow collision waves ending by the ejection of several solitons along with multiple dispersive waves, thus generating a broad supercontinuum ranging from 500 to 1200 nm.

IV. SOLITON CHAINS

To demonstrate the generality of the realization of the TOD-driven NC dynamics in soliton arrays, we here consider the input in the form of a "prefabricated" chain of ten identical solitary pulses with temporal width $T_0 = 10$ fs, peak power $P_0 = 262.5$ W, and separation $\Delta T = 5T_0$ between them. The chain is represented by the following input:

$$u_0(T) = \sqrt{P_0}\, \mathrm{sech}\left(\frac{T}{T_0}\right) \exp(-i\,\omega_k T)$$
$$+ \sqrt{P_0} \sum_{n=2}^{10} \mathrm{sech}\left(\frac{T + n\Delta T}{T_0}\right). \quad (4)$$

Fixing the TOD coefficient here as $\beta_3 = 3.5 \times 10^{-5}$ ps^3/m, a negative frequency shift ("kick") ω_k is applied to the leftmost soliton in the chain, to initiate the NC dynamical regime, in analogy to the classical realization of the NC in mechanics. The result is displayed in Figs. 8(a)–8(c) for the zero, weak ($\omega_k = -30$ ps^{-1}), and strong ($\omega_k = -200$ ps^{-1}) kicks, respectively. In addition, in Fig. 9 another case is shown, when a relatively strong kick ($\omega_k = +100$ ps^{-1}) is applied, in the opposite direction, to the rightmost soliton in the chain.

The asymmetry imposed by the TOD provides energy and momentum transfer along the chain, from left to right, through
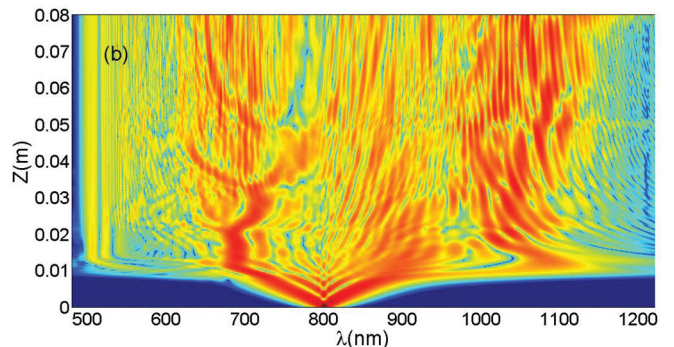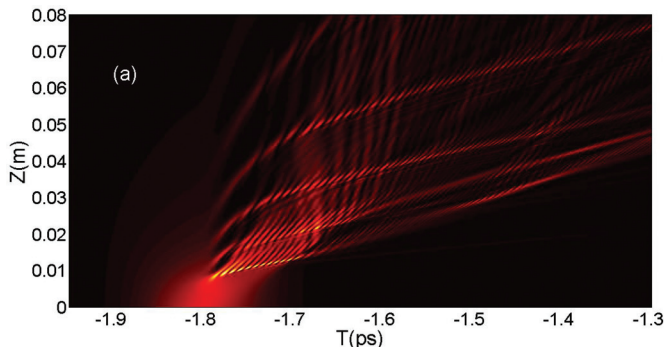

FIG. 7. (Color online) The fission of the 50-soliton, as seen in the temporal (a) and spectral (b) domains, with the subsequent formation of the Newton's cradle and ejection of multiple solitons. The simulation was performed in the framework of the full equation (1), including the Raman and self-steepening nonlinear terms, and the higher-order dispersive terms of up to the seventh order (see details in the text).
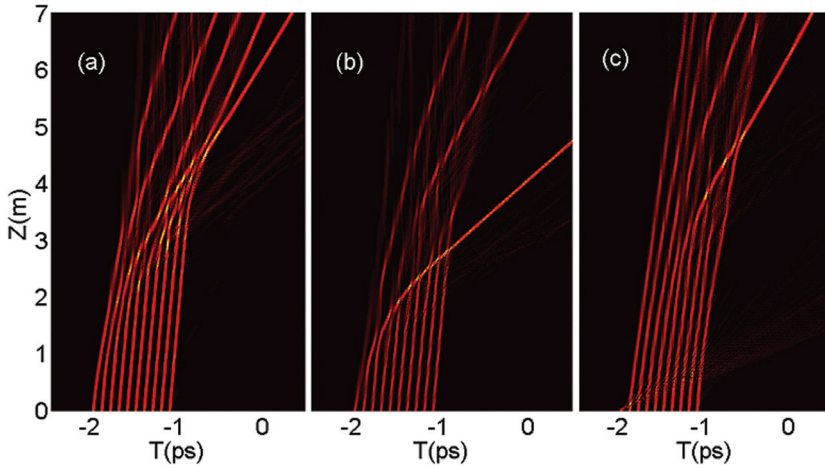
FIG. 8. (Color online) The dynamics of the chain of ten identical solitons, built as per Eq. (4), under the action of the TOD, with $\beta_3 = 3.5 \times 10^{-5}$ ps^3/m, and the initial kick applied to the leftmost soliton: (a) $\omega_k = 0$ (no kick); (b) $\omega_k = -30$ ps^{-1} (a weak kick); (c) $\omega_k = -200$ ps^{-1} (a strong kick).

quasielastic repulsive collisions between the solitons [30], even without any kick originally applied to the leftmost soliton [see Fig. 8(a)]. It is relevant to mention that the initial chain (4) is built of in-phase solitons. However, the analysis of numerical data demonstrates that, as a result of the TOD-induced asymmetry, there appear phase shifts between adjacent solitons in the chain, and, at the evolution stage when soliton collisions take place, the phase shifts attain values between $\pi/2$ and $3\pi/2$, similar to the NC formed by the TOD-driven fission of the N solitons (see above). Even in the absence of the initial kick, Fig. 8(a) demonstrates a dynamical regime which resembles the NC dynamics in the soliton chains which was observed above, namely, the propagation of a narrow collision wave through the chain, that ends up by the ejection of a fast soliton. The characteristic features of the NC dynamics become more prominent under the action of the initial kick [see Fig. 8(b)]. The situation is, however, different when the first soliton is set in motion by a strong kick. The initial violent collision leads to rapid destruction of the incident soliton [see Fig. 8(c)], and the chain subsequently demonstrates a less pronounced quasi-NC regime, more similar to that in the absence of the kick [cf. Fig. 8(a)]. Thus, dealing with the chain of identical solitons, we conclude that there exists a range of values of the initial kick which gives rise to the most well-pronounced NC behavior. On the other hand, it is relevant to mention that taking β_3 twice as large as in these simulations produces a picture which, without any kick, is quite similar to the one generated by the applied kick in Fig. 8(b).

Kicking the rightmost soliton in the opposite direction leads to its collision with the neighbor and their merger into a single soliton. After that, the NC develops in essentially the same form as in the absence of the kick (see Fig. 9).

For emulating the NC structure, the initial periodic pattern does not need to be built as a chain of solitons. As Fig. 10 shows, one can use as an input simply a truncated cosinusoidal wave, $u_0(T) = \sqrt{P_0}\cos(T/\tilde{T}_0)$. The NC dynamics, resulting in the final release of the accelerated soliton with an enhanced power, is well observed in this case too.

Lastly, it is relevant to mention that a recently investigated regime of the evolution of the input in the form of a truncated Airy function, $u_0(T) = A_0\mathrm{Ai}(T)\exp(aT)$, in the framework of the integrable NLS equation (without the TOD term), which gives rise to ejection of individual solitons from the Airy pattern [33], also demonstrates features similar to those expected from the NC dynamics in a multipulse chain. Another relevant example is provided by recent works which simulated the splitting of a broad input into soliton arrays in models with the quadratic (second-harmonic-generating nonlinearity) [34]: In some cases, they display the release of Cherenkov wave packets, which resemble the ejection of the free soliton from the NC soliton array, which was reported above.
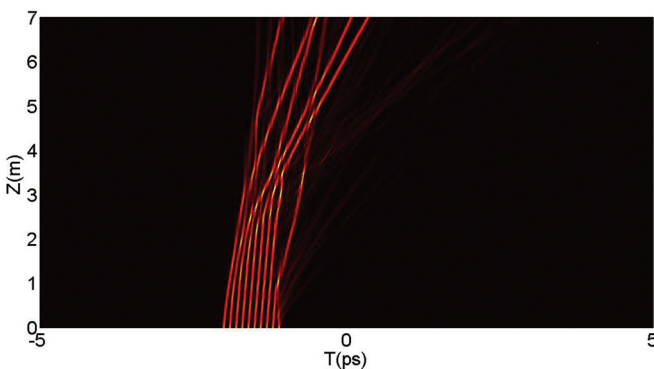

FIG. 9. (Color online) The same as in Fig. 8, but when kick $\omega_k = +100$ ps^{-1} is applied to the rightmost soliton in the initial soliton array.
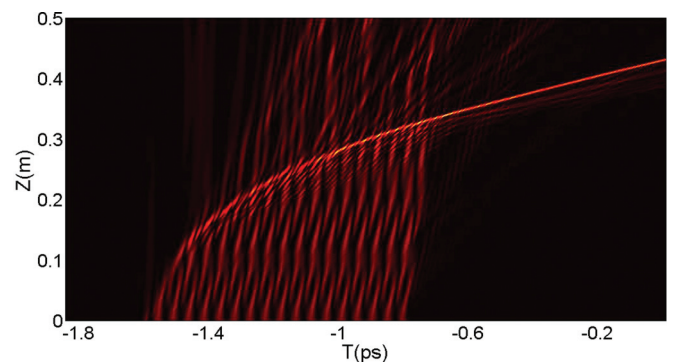

FIG. 10. (Color online) The NC emulated by launching as an input a cosinusoidal wave. The truncation of the input was done at the time interval of about 0.8 ps. This simulation was performed with TOD coefficient $\beta_3 = 6.98 \times 10^{-5}$ ps^3/m.

V. CONCLUSION

We have introduced the optical analog of the NC (Newton's cradle) in the form of soliton arrays, or chains of optical pulses. The characteristic feature of the NC, i.e., the transmission of a narrow wave of collisions, which is realized as the passage of the tallest soliton through the whole array, from left to right, is driven by the TOD, and ends by release of the tallest soliton, with a conspicuous frequency shift. Due to inelasticity of soliton collisions under the action of TOD, the passing soliton collects energy in the course of its motion through the array. We have demonstrated that the NC, built of optical pulses with different amplitudes, is naturally generated by the TOD-driven fission of N-solitons. Similar NC dynamical regimes are induced as well by the TOD acting on arrays of identical solitons. For N large enough, the NC may support the multiple passage and eventual ejection of solitons with enhanced power, through their consecutive collisions with other pulses that stay bound in the long chain. Along with multiple dispersive waves emitted the ejected solitons generate a broadband supercontinuum. The NC-forming mechanism is robust against the inclusion of the Raman and self-steepening effects, as well as dispersion terms of order higher than three.

While the similarity of the dynamical regimes reported above to the classical mechanical NC is far from being exact, the features demonstrated by the arrays of solitons suggest that the original NC concept may be extended for nonlinear-wave settings, acquiring new properties: The soliton arrays building the NC as a result of the fission of N-soliton input are naturally nonuniform, and the tallest soliton, moving across the array, effectively passes through other solitons, which is possible for quasiparticles but impossible for hard beads in the mechanical NC. Furthermore, the passing soliton collects the energy and momentum from other solitons, and is eventually released along with conspicuous amounts of radiation, which lends the NC dynamics in soliton arrays novel inelastic features. The dynamical regimes that proceed via the formation of the soliton NCs may find applications in optics, such as optimization of the supercontinuum generation.

It is expected that soliton-based NCs may also be constructed in other models of nonlinear optics, such as chains of gap solitons in Bragg gratings or photonic crystals. In particular, the breakup of higher-order spatial solitons under the action of nonlinear absorption, demonstrated in Ref. [35], may be related to this phenomenology.

[1] E. J. Hinch and S. Saint-Jean, Proc. R. Soc. London, Ser. A **455**, 3201 (1999); V. Ceanga and Y. Hurmuzlu, ASME J. Appl. Mech. **68**, 575 (2001); P. Zamankhan and M. H. Bordbar, *ibid.* **73**, 648 (2006); S. Hutzler, G. Delaney, D. Weaire, and F. MacLeod, Am. J. Phys. **72**, 1508 (2004); C. M. Donahue, C. M. Hrenya, R. H. Davis, K. J. Nakagawa, A. P. Zelinskaya, and G. G. Joseph, J. Fluid Mech. **650**, 479 (2010).

[2] R. Cross, Phys. Teach. **50**, 206 (2012).

[3] H. Arnolds, C. E. M. Rehbein, G. Roberts, R. J. Levis, and D. A. King, J. Phys. Chem. B **104**, 3375 (2000); T. Kinoshita, T. R. Wenger, and D. S. Weiss, Nature (London) **440**, 900 (2006); S. Wüster, C. Ates, A. Eisfeld, and J. M. Rost, Phys. Rev. Lett. **105**, 053004 (2010).

[4] D. Novoa, B. A. Malomed, H. Michinel, and V. M. Perez-Garcia, Phys. Rev. Lett. **101**, 144101 (2008).

[5] B. A. Malomed, V. A. Oboznov, and A. V. Ustinov, Zh. Eksp. Teor. Fiz. (Sov. Phys. JETP) **97**, 924 (1990); B. A. Malomed and V. A. Ustinov, J. Appl. Phys. **67**, 3791 (1990).

[6] V. Besse, H. Leblond, D. Mihalache, and B. A. Malomed, Phys. Rev. E **87**, 012916 (2013).

[7] Yu. S. Kivshar and B. A. Malomed, Rev. Mod. Phys. **61**, 763 (1989).

[8] J. Satsuma and N. Yajima, Prog. Theor. Phys. Suppl. **55**, 284 (1974).

[9] H. Sakaguchi and B. A. Malomed, Phys. Rev. E **70**, 066613 (2004); H. Yanay, L. Khaykovich, and B. A. Malomed, Chaos **19**, 033145 (2009).

[10] R. H. Stolen, L. F. Mollenauer, and W. J. Tomlinson, Opt. Lett. **8**, 186 (1983).

[11] F. Salin, P. Grangier, G. Roger, and A. Brun, Phys. Rev. Lett. **56**, 1132 (1986); **60**, 569 (1988).

[12] R. Driben and B. A. Malomed, Europhys. Lett. **99**, 54001 (2012).

[13] E. A. Golovchenko, E. M. Dianov, A. M. Prokhorov, and V. N. Serkin, JETP Lett. **42**, 74 (1985).

[14] Y. Kodama and A. Hasegawa, IEEE Photonics Technol. Lett. **QE-23**, 510 (1987).

[15] J. Herrmann, U. Griebner, N. Zhavoronkov, A. Husakou, D. Nickel, J. C. Knight, W. J. Wadsworth, P. St. J. Russell, and G. Korn, Phys. Rev. Lett. **88**, 173901 (2002).

[16] W. Liu, L. Pang, X. Lin, R. Gao, and X. Song, Appl. Opt. **51**, 8095 (2012).

[17] F. M. Mitschke and L. F. Mollenauer, Opt. Lett. **11**, 659 (1986).

[18] J. P. Gordon, Opt. Lett. **11**, 662 (1986).

[19] K. J. Blow and D. Wood, IEEE J. Quantum Electron. **25**, 2665 (1989).

[20] Y. S. Kivshar and G. P. Agrawal, *Optical Solitons: From Fibers to Photonic Crystals* (Academic Press, San Diego, 2003); G. P. Agrawal, *Nonlinear Fiber Optics*, 4th ed. (Academic Press, New York, 2007).

[21] J. M. Dudley, G. Gentry, and S. Coen, Rev. Mod. Phys. **78**, 1135 (2006); D. V. Skryabin and A. V. Gorbach, *ibid.* **82**, 1287 (2010).

[22] E. M. Dianov, Z. S. Nikonova, A. M. Prokhorov, and V. N. Serkin, Sov. Tech. Phys. Lett. **12**, 311 (1986).

[23] C. M. Chen and P. L. Kelley, J. Opt. Soc. Am. B **19**, 1961 (2002).

[24] W. H. Reeves, D. V. Skryabin, F. Biancalana, J. C. Knight, P. St. J. Russell, F. Ominetto, A. Efimov, and A. J. Taylor, Nature (London) **424**, 511 (2003); J. H. Lee, J. V. Howe, C. Xu, and

X. Liu, IEEE J. Sel. Top. Quantum Electron. **14**, 713 (2008); S. Kivistö, T. Hakulinen, M. Guina, and O. G. Okhotnikov, IEEE Photon. Technol. Lett. **19**, 934 (2007).

[25] R. R. Alfano and S. L. Shapiro, Phys. Rev. Lett. **24**, 592 (1970); J. C. Knight, T. A. Birks, P. St. J. Russell, and D. M. Atkin, Opt. Lett. **21**, 1547 (1996); J. K. Ranka, R. S. Windeler, and A. J. Stentz, *ibid.* **25**, 25 (2000); J. C. Knight, Nature (London) **424**, 847 (2003); K. L. Corwin, N. R. Newbury, J. M. Dudley, S. Coen, S. A. Diddams, K. Weberand, and R. S. Windeler, Phys. Rev. Lett. **90**, 113904 (2003); Z. Zhu and T. G. Brown, Opt. Express **12**, 689 (2004); M. H. Frosz, P. Falk, and O. Bang, *ibid.* **13**, 6181 (2005); P. Falk, M. H. Frosz, and O. Bang, *ibid.* **13**, 7535 (2005); A. Efimov and A. J. Taylor, *ibid.* **16**, 5942 (2008); R. Driben, A. Husakou, and J. Herrmann, Opt. Lett. **34**, 2132 (2009); R. Driben and N. Zhavoronkov, Opt. Express **18**, 16733 (2010).

[26] J. C. Travers, W. Chang, J. Nold, N. Y. Joly, and P. St. J. Russell, J. Opt. Soc. Am. B **28**, A11 (2011); M. F. Saleh, W. Chang, P. Holzer, A. Nazarkin, J. C. Travers, N. Y. Joly, P. St. J. Russell, and F. Biancalana, Phys. Rev. Lett. **107**, 203902 (2011); M. Azhar, G. K. L. Wong, W. Chang, N. Y. Joly, and P. St. J. Russell, Opt. Express **21**, 4405 (2013).

[27] N. Akhmediev and M. Karlsson, Phys. Rev. A **51**, 2602 (1995).

[28] I. M. Besieris and A. M. Shaarawi, Phys. Rev. E **78**, 046605 (2008).

[29] P. K. A. Wai, H. H. Chen, and Y. C. Lee, Phys. Rev. A **41**, 426 (1990).

[30] M. N. Islam, G. Sucha, I. Bar-Joseph, M. Wegener, J. P. Gordon, and D. S. Chemla, J. Opt. Soc. Am. B **6**, 1149 (1989); B. J. Hong and C. C. Yang, *ibid.* **8**, 1114 (1991); B. A. Malomed, Phys. Rev. A **44**, 1412 (1991); R. Driben and B. A. Malomed, Opt. Commun. **197**, 481 (2001); A. Peleg, M. Chertkov, and I. Gabitov, Phys. Rev. E **68**, 026605 (2003); F. Luan, D. V. Skryabin, A. V. Yulin, and J. C. Knight, Opt. Express **14**, 9844 (2006); M. H. Frosz, O. Bang, and A. Bjarklev, *ibid.* **14**, 9391 (2006); N. Akhmediev, J. M. Soto-Crespo, and A. Ankiewicz, Eur. Phys. J. Special Topics **185**, 259 (2010).

[31] S. Linden, H. Giessen, and J. Kuhl, Phys. Status Solidi B **206**, 119 (1998).

[32] A. Efimov, A. V. Yulin, D. V. Skryabin, J. C. Knight, N. Joly, F. G. Omenetto, A. J. Taylor, and P. Russell, Phys. Rev. Lett. **95**, 213902 (2005); R. Driben, F. Mitschke, and N. Zhavoronkov, Opt. Express **18**, 25993 (2010); A. Demircan, Sh. Amiranashvili, and G. Steinmeyer, Phys. Rev. Lett. **106**, 163901 (2011); R. Driben and I. Babushkin, Opt. Lett. **37**, 5157 (2012); A. Demircan, S. Amiranashvili, C. Brie, C. Mahnke F. Mitschke and G. Steinmeyer, Sci. Rep. **2**, 850 (2012).

[33] Y. Fattal, A. Rudnick, and D. M. Marom, Opt. Express **19**, 17298 (2011).

[34] M. Bache, O. Bang, B. B. Zhou, J. Moses, and F. W. Wise, Opt. Express **19**, 22557 (2011); H. Guo, X. Zeng, B. Zhou, and M. Bache, J. Opt. Soc. Am. B **30**, 494 (2013).

[35] O. Katz, Y. Lahini, and Y. Silberberg, Opt. Lett. **33**, 2830 (2008).